Available online at www.sciencedirect.com
ScienceDirect
Journal of Molecular Catalysis A: Chemical 286 (2008) 63–69
JOURNAL OF MOLECULAR CATALYSIS A: CHEMICAL
www.elsevier.com/locate/molcata

Zn- and La-modified TiO_2 photocatalysts for the isomerization of norbornadiene to quadricyclane

Ji-Jun Zou, Bin Zhu, Li Wang *, Xiangwen Zhang, Zhentao Mi

Key Laboratory for Green Chemical Technology of Ministry of Education, School of Chemical Engineering and Technology, Tianjin University, 92 Weijing Road, Tianjin 300072, PR China

Received 24 November 2007; received in revised form 17 January 2008; accepted 22 January 2008
Available online 12 February 2008

Abstract

Zn-doped and La/Zn co-doped TiO_2 nanoparticles were prepared by sol–gel method and utilized as the photocatalysts for the isomerization of norbornadiene to quadricyclane that has significant potential for solar energy storage and high-energy fuel synthesis. For Zn-doped samples, Zn ions do not enter the TiO_2 lattice, but distribute on the particle surface in the form of ZnO crystallites. These crystallites inhibit the agglomeration, growth and anatase-to-rutile phase transformation of TiO_2. The prepared particles contain considerable amount of surface-bound OHs, especially for 1%Zn/TiO_2. A red shift in the optical absorption is observed due to the electron transfer between TiO_2 and ZnO. In the photocatalytic isomerization reaction, Zn-doped TiO_2 exhibits higher activity than homogenous sensitizer like Ethyl Michler's Keton, and 1%Zn/TiO_2 produces the highest yield of quadricyclane. To further enhance the activity, 1%Zn/TiO_2 was co-doped with La. La_2O_3 crystallites also distribute on the surface of TiO_2, similar to the case of ZnO. The particle size is reduced to <7 nm but the surface-bound OHs are decreased to some degree. There is a significant blue shift in the optical absorption with a sharply increased absorbance in the UV region due to the quantum-size effect. 5%La–1%Zn/TiO_2 and 3%La–1%Zn/TiO_2 exhibit higher activity compared with 1%Zn/TiO_2, but higher or lower content of La is detrimental to the reaction. It is concluded that doping Zn can significantly increase the surface-bound OHs, whereas doping La reduces the particle to quantum-size at the expense of surface-bound OHs. A good compromise between the two factors eventually provides a high activity. The isomerization reaction over semiconductors is proposed to proceed through an exciplex (charge-transfer) intermediate.

Keywords: Norbornadiene; Quadricyclane; Isomerization; Doping; TiO_2

1. Introduction

Photocatalytic isomerization of norbornadiene(NBD) to quadricyclane (QC) has attracted much attention due to its promising potential in solar energy storage and conversion. When NBD is transformed to QC under irradiation, energy of about 89 kJ/mol is stored in the highly strained molecules, which can be released thermally through the reversed transformation of QC to NBD [1–4]. Recently, QC has also been identified as a potential high-energy replacement for, or additive to, current hydrocarbon-based rocket propellants, because the extraordinary high strain energy offers a very high specific impulse. It has been reported that QC-based fuels provide more propulsion than the widely used kerosene fuels such as RP-1 [5–7]. As a non-toxic high-energy fuel, QC is also designed for satellite propulsion system to replace highly toxic fuels like hydrazine and nitrogen tetroxide [8]. Moreover, QC is thermally and chemically stable, which means that it can be easily stored and transported like other hydrocarbon fuels.

The isomerization of NBD to QC shows extremely low efficiency in the absence of sensitizers due to the poor optical absorbance of NBD molecules. With the presence of sensitizers, the reaction occurs through the triplet state of NBD. The sensitizers are excited to the triplet state (^{3}S) under irradiation, which subsequently transfer the energy to NBD molecules to form the triplet state (^{3}NBD). Then the ^{3}NBD undergoes adiabatic isomerization to form the triplet state of Q (^{3}QC) which very rapidly decays to the ground state to produce QC. It has been reported that sensitizers including benzophenone, unsubstituted and substituted Michler's Ketones, and various transient metal complexes such as Cu salts and Rh compounds are very

* Corresponding author. Tel.: +86 22 27892340; fax: +86 22 27402604.
E-mail addresses: jj_zouchem@yahoo.com.cn (J.-J. Zou), wlytj@yahoo.com.cn (L. Wang).

1381-1169/$ – see front matter © 2008 Elsevier B.V. All rights reserved.
doi:10.1016/j.molcata.2008.01.045

effective [9–14]. However, these sensitizers suffer from some drawbacks. First, the homogenous sensitizers are soluble in the reaction system, which causes difficulties in product purification and sensitizers recycling. Second, the sensitizers are prone to decomposition under irradiation. With these regards, heterogeneous photocatalysts, instead of homogenous sensitizers, are more favorable. To the authors' knowledge, however, there is only one attempt to use ZnO as the photocatalyst for this reaction [15].

Heterogeneous semiconductors have been extensively used for many photocatalytic reactions such as organics degradation and hydrogen production, among which TiO_2 is widely used owing to its low-cost, non-toxicity, chemical and biological inertness, and photostability [16–18]. However, the activity of TiO_2 needs to be improved due to the low optical absorbance and high charge–hole recombination rate. To overcome these problems, doping and surface deposition have been widely studied. Specifically, doping of Zn and La has been reported to enhance the photocatalytic performance of TiO_2 [19–26], but co-doping of Zn and La is not found in literature. In this work, Zn-doped TiO_2 nanoparticles were prepared using sol–gel method. The crystal structure, surface chemical state, and optical absorption of the materials were characterized. The optimal Zn content was determined for the photocatalytic isomerization of NBD to QC. Then co-doping of La and Zn were conducted to further improve the activity. The factors influencing the photocatalytic performance and possible mechanism were discussed.

2. Experimental

2.1. Preparations

All the chemicals used in the experiments were reagent grade and used as received without further purification. $Ti(SO_4)_2$, $ZnSO_4$ and $La(NO_3)_3$ were used as the sources of Ti, Zn and La, respectively. Types of nanoparticles including Zn-doped TiO_2 (hereafter denoted as Zn/TiO_2), Zn and La co-doped TiO_2 (hereafter denoted as $La–Zn/TiO_2$), and naked TiO_2 and ZnO were prepared. To prepare these materials, one or more salts with defined proportion (in mole) were dissolved in deionized water. Then $NH_3{\cdot}H_2O$ was added dropwise (1–2 mL/min) under vigorous stirring until the pH of the solution reached 7. The resulting sol was aged at room temperature for 4 h. The obtained gel was dried at 100 °C for 8 h and ultimately calcined at 500 °C or 700 °C in air for 3 h.

2.2. Characterizations

XRD characterizations were conducted at room temperature using a D/MAX-2500 X-ray diffractometer equipped with Cu Kα radiation at 40 kV and 140 mA. TEM observations were carried out with a Tecnai G^2 F-20 transmission electron microscope. N_2 physical adsorptions were performed with a Gemini V instrument, and the specific surface area was calculated using the multi-plot method. XPS characterizations were conducted with a PerkinElmer PHI-1600 X-ray photoelectron spectroscope equipped with Al Kα radiation (1486.6 eV). The binding energy was calibrated using the C_{1s} peak (284.6 eV) of contaminant carbon. UV–vis diffuse reflectance spectra were recorded with a JASCO V-570 spectrometer using $BaSO_4$ plate as the reference.

2.3. Photocatalytic reactions

The photocatalytic isomerization of NBD to QC was carried out in an inner irradiation quartz reactor with a volume of 250 mL. A 400 W high-pressure Hg lamp with outside water-cooling was used as the irradiation source. The reactant mixture contained 10 mL of NBD and 0.3 g of photocatalyst powders suspended in 220 mL of dimethyl benzene by a magnetic stirrer. The reaction was conducted for 5 h and a sample was withdrawn each hour for analysis. The samples were analyzed using a HP 4890 chromatograph equipped with a BP-1 capillary column (25 m × 0.33 mm × 0.05 μm) with N_2 as the carrier gas and FID as the detector.

3. Results and discussion

3.1. Zn-doped TiO_2 nanoparticles

3.1.1. Crystal structures

Fig. 1 shows the XRD patterns of Zn/TiO_2 calcined at 500 °C. All the samples exhibit six diffraction peaks at 25.3°, 7.8°, 47.9°, 53.8°, 55.0°, and 62.7°, which are assigned to the (1 0 1), (0 0 4), (2 0 0), (1 0 5), (2 1 1) and (2 0 4) faces of anatase TiO_2, respectively. Doping Zn does not produce any new diffraction peaks. Table 1 shows that the cell parameters of doped TiO_2 are very similar to those of naked TiO_2. These results suggest that Zn ions do not enter the TiO_2 lattices to substitute Ti ions, because the substitution of smaller Ti ion (68 pm) by bigger Zn ion (74 pm) should induce increase in lattice parameters and shift in diffraction patterns. Meanwhile, no separate ZnO phases are observed even though the molar percentage of Zn reaches 5%. Therefore, ZnO should be highly dispersed on the surface of TiO_2 nanopar-

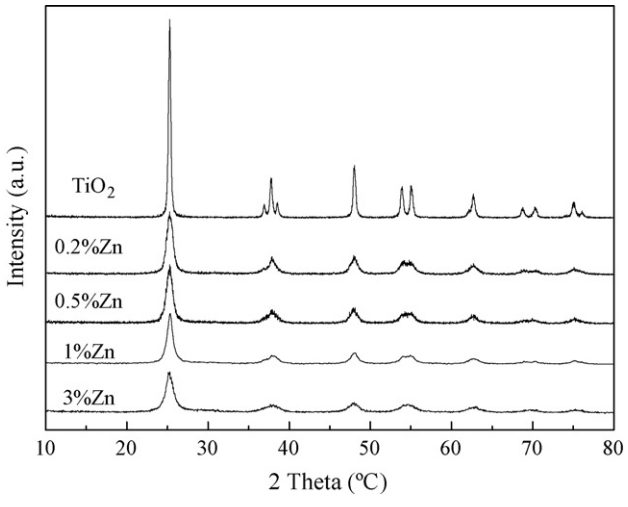

Fig. 1. XRD patterns of TiO_2 and Zn/TiO_2 calcined at 500 °C.

Table 1
Crystal structure and specific surface area of TiO_2 and Zn/TiO_2 derived from XRD and N_2-adsorption

Samples	Calcination temperature (°C)	Grain size (nm)	Lattice parameters		BET specific surface area (m^2/g)
			a (nm)	*c* (nm)	
TiO_2	500	14.7	3.7852	9.5139	38.8
0.2%Zn/TiO_2	500	8.2	3.7876	9.4842	106.2
0.5%Zn/TiO_2	500	7.6	3.7897	9.4974	100.9
1%Zn/TiO_2	500	8.1	3.7840	9.4301	84.9
3%Zn/TiO_2	500	9.6	3.7873	9.4912	55.4
TiO_2	700	22.0	3.7881	9.5289	25.5
0.5%Zn/TiO_2	700	19.0	3.7851	9.5105	41.1
1%Zn/TiO_2	700	20.6	3.7861	9.5089	30.1
3%Zn/TiO_2	700	19.7	3.7876	9.4973	34.7

ticles or between the interfaces of TiO_2 agglomerates in form of crystallites. The diffraction peaks of TiO_2 become broader and weaker after doping Zn, indicative of reduced grain size and low extent of crystallinity. This suggests that doping Zn suppresses the growth and crystallization of TiO_2 nanoparticles. Table 1 also summarizes the grain size calculated according to the Scherer equation. The naked TiO_2 is 14.7 nm, while the doped particles have much smaller size (less than 10 nm). As a result, the doped TiO_2 has significantly higher specific surface area, as shown in Table 1.

Fig. 2 shows the XRD patterns of Zn/TiO_2 calcined at 700 °C. The intensity of the diffraction peaks goes up with increasing calcination temperature, indicative of the enhanced crystallization. A new peak at 27.5° appears in the patterns of naked TiO_2, which is assigned to the (1 1 0) face of rutile phase. This is the evidence of phase transformation from anatase to rutile. However, Zn-doped particles do not have such a peak, indicating that doping Zn inhibits this phase transformation.

Fig. 3 shows the TEM images of naked and doped TiO_2 calcined at 500 °C. The size of Zn-doped TiO_2 is about 10 nm, in good agreement with the XRD result. However, the size of naked TiO_2 observed by TEM is about 20 nm, much bigger than that derived from XRD analysis. This suggests that TiO_2 particles tend to aggregate with each other to form bigger particles, and doping Zn effectively inhibits this agglomeration.

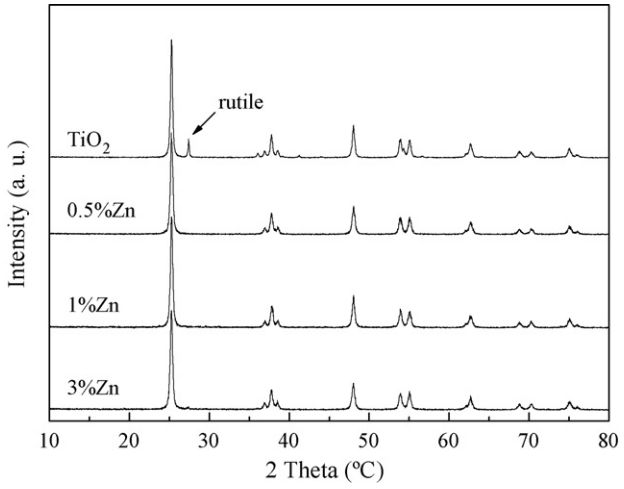

Fig. 2. XRD patterns of TiO_2 and Zn/TiO_2 calcined at 700 °C.

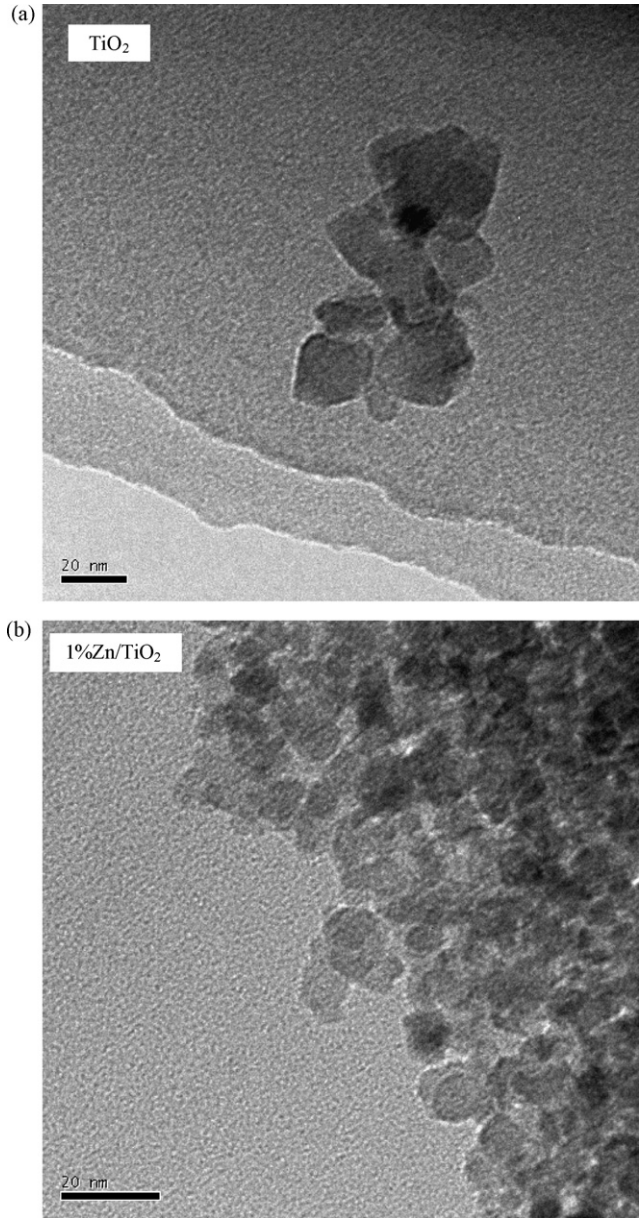

Fig. 3. TEM images of (a) TiO_2 and (b) 1%Zn–TiO_2 calcined at 500 °C.

Table 2
Surface properties of TiO_2 and Zn/TiO_2 derived from XPS characterizations

Samples	Calcination temperature (°C)	Atomic surface concentration			Percentage of surface oxygen	
		Ti	Zn	Zn/Ti	O1s (Ti-O)	O1s (–OH)
TiO_2	500	16.2	–	–	63.8	36.2
0.5%Zn/TiO_2	500	13.2	0.2	0.02	54.4	45.6
0.5%Zn/TiO_2	700	11.3	0.7	0.06	43.8	36.2
1%Zn/TiO_2	500	15.0	2.1	0.14	44.5	55.5
1%Zn/TiO_2	700	12.7	1.0	0.07	57.2	42.8
3%Zn/TiO_2	500	16.4	2.4	0.15	53.8	46.2
5%Zn/TiO_2	500	15.5	2.6	0.16	55.3	44.7

3.1.2. Surface properties

XPS characterizations show that the Ti2p spectrum of doped TiO_2 (Figure not shown) exhibits two peaks at 458.4 eV and 464.0 eV assigned to the two spin-orbit components of $Ti2p_{3/2}$ and $Ti2p_{1/2}$. The positions of these peaks are in accord with those of naked TiO_2, and the relative intensity ratio of them is close to the theoretical value of 2. The Zn2p spectrum exhibits two peaks at 1021.5 eV and 1044.7 eV, which are also consistent with those of typical ZnO. These results provide evidence that Zn ions do not enter TiO_2 lattice but exist in individual phases. Table 2 summarizes the atomic concentration of Ti, O and Zn obtained from XPS analysis. The Zn/Ti atomic ratio is significantly higher than the defined value, indicating concentrated Zn on the particle surface. It confirms that most of the ZnO crystallites distribute on the surface of TiO_2 nanoparticles.

The segregation of ZnO on the surface of TiO_2 nanoparticles is probably due to the difference in the hydrolysis rate and diameter of Ti^{4+} and Zn^{2+} ions. It has been recently reported that the agglomeration of TiO_2 particles plays important role in the growth of particles, and the anatse-to-rutile phase transformation easily occurs at the interface of agglomerates [27]. Doping Zn on surface can avoid the direct contact of TiO_2 particles, thereby retarding the agglomeration. As a result, the particle growth and anatase-to-rutile phase transformation are inhibited, as testified by XRD and TEM characterizations.

Fig. 4 shows the O1s XPS spectra of doped and naked TiO_2. The broad and asymmetric peaks indicate that there are at least two types of oxygen species on the surface. Fitting of the curves gives two components centered at 529.6 eV and 531.5 eV, which are assigned to lattice oxygen (O–Ti) and surface-bound hydroxyl groups (OHs), respectively [20]. Their relative content is also summarized in Table 2. It can be seen that, doping Zn significantly increases the content of surface-bound OHs. Specifically, 1%Zn/TiO_2 calcined at 500 °C exhibits the highest content of surface-bound OHs.

3.1.3. Optical absorption

Fig. 5 shows the UV–vis diffuse reflectance spectra of doped and naked TiO_2 nanoparticles. All the doped samples show extended red shift and enhanced absorbance in the visible range. The maximum absorption and absorption band edge are 327 nm and 400 nm for naked TiO_2, whereas they are 348 nm and 410 nm for 1%Zn/TiO_2, respectively. The red shift in the range of 200–420 nm can be attributed to the charge transition between the zinc ion *d* electrons and the TiO_2 conduction or valence band [21]. The increased absorption in the region of 420–600 nm is attributed to the sub-band transitions relative to surface-bound OHs [20]. In this range, 1%Zn/TiO_2 has the maximum absorption, in agreement with its highest OHs content.

3.1.4. Photoactivity

Fig. 6 shows the activity of NBD isomerization to QC over TiO_2, ZnO and Zn/TiO_2. Since the selectivity of this reaction is 100%, the yield of QC is used to evaluate the performance

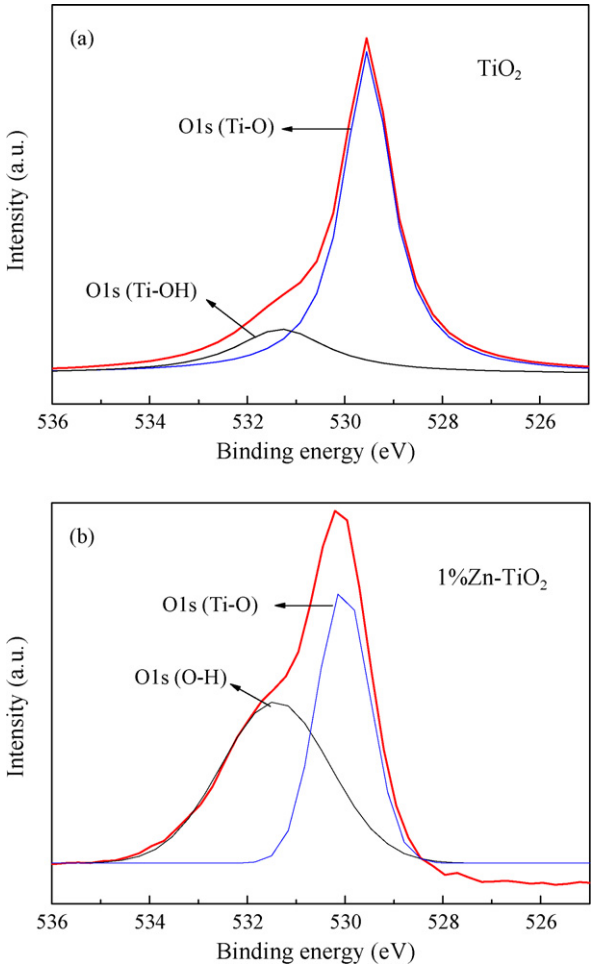

Fig. 4. Fitted O1s XPS spectra of (a) TiO_2 and (b) 1%Zn/TiO_2 calcined at 500 °C.

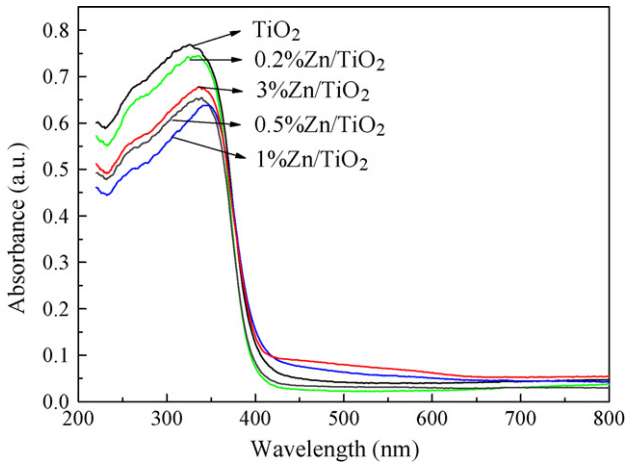

Fig. 5. Optical absorption of TiO_2 and Zn/TiO_2 calcined at 500 °C.

of photocatalysts. The reaction does not occur in the absence of photocatalyst. Naked TiO_2 and ZnO semiconductors can catalyze the reaction but the activity is relatively low, with the yield of QC as 54.1% and 39.1% in 5 h, respectively. Doping Zn in TiO_2 significantly improves the activity. $1\%Zn/TiO_2$ shows the highest yield of 74.1%, and $0.5\%Zn/TiO_2$ and $3\%Zn/TiO_2$ exhibit similar activity. The improvement of activity by doping Zn may be attributed to the following factors. First, there is a great quantity of surface-bound OHs on the surface of Zn/TiO_2 catalysts. Many studies have demonstrated that the surface-bound OHs play a very important role in photocatalytic reactions [16,17]. Second, the particle size of TiO_2 is greatly reduced, which enhances the photoinduced charge transfer from the bulk of particles to the surface-absorbed reactants. The large surface area also provides more absorbing sites for reactant molecules. Since $1\%Zn/TiO_2$ has the best properties in terms of surface-bound OHs and specific surface area, it is natural that this photocatalyst shows the best performance. Fig. 6 also shows that calcination photocatalyst at higher temperature is detrimental to the reaction because the above-mentioned properties are impaired.

It is noticed that doped TiO_2 shows activity higher than homogenous sensitizers such as Ethyl Michler's Keton. Cahill and Steppel disclosed the isomerization of pure NBD using a 400 W iron halide-doped lamp as the irradiation source and 3.86 wt.% of 4,4′-bis(diethylamino)benzophenone as the sensitizer [14]. In 5 h, the average conversion rate of NBD is about 1.1 g/g_{catal} h. During the same duration, $1\%Zn–TiO_2$ prepared in the present work shows an average conversion rate of 4.3 g/g_{catal} h. We also evaluated the activity of this sensitizer under the conditions identical to TiO_2-based photocatalysts, and got an average conversion rate of 4.2 g/g_{catal} h. This result clearly shows that the TiO_2-based photocatalysts are active enough to replace the homogenous sensitizers.

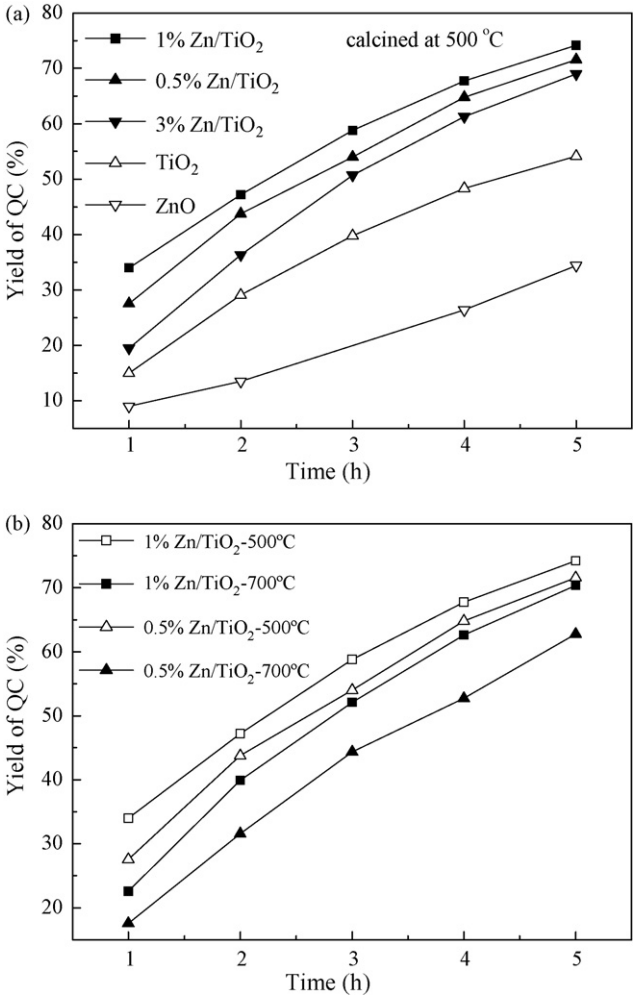

Fig. 6. Photocatalytic activity of (a) TiO_2, ZnO and Zn/TiO_2 calcined at 500 °C, and (b) Zn/TiO_2 calcined at different temperatures.

3.2. *La and Zn co-doped TiO_2 nanoparticles*

3.2.1. *Characterization results*

Co-doping of La and Zn was conducted to further improve the activity of $1\%Zn/TiO_2$. As shown in Fig. 7, doping La does not cause any shift in diffraction angles, indicating that La ions do not enter the TiO_2 lattice and exist as small crystallites on the particle surface, similar to the case of doping Zn. How-

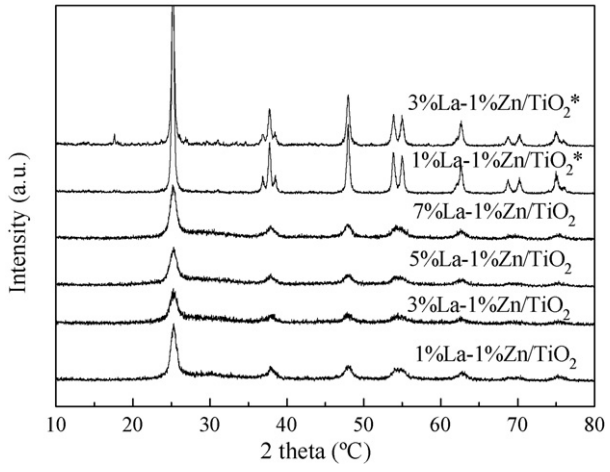

Fig. 7. XRD patterns of La and Zn co-doped TiO_2. (Samples with asterisk were calcined at 700 °C; the others were calcined at 500 °C.)

Table 3
Grain size of La and Zn co-doped TiO_2 calcined at 500 °C

Samples	Grain size (nm)
1%La–1%Zn	7.6
3%La–1%Zn	6.9
5%La–1%Zn	6.5
7%La–1%Zn	6.2

Table 4
Surface properties of Zn and La co-doped TiO_2 calcined at 500 °C

Samples	Atomic surface concentration ratio		Percentage of OHs (%)
	Zn/Ti	La/Ti	
1%La–1%Zn/TiO_2	0.04	0.06	42.0
3%La–1%Zn/TiO_2	0.03	0.11	41.3
5%La–1%Zn/TiO_2	0.03	0.15	40.8
7%La–1%Zn/TiO_2	0.02	0.19	37.1

ever, the diffraction peaks are widened and weakened compared with 1%Zn%TiO_2, suggesting that doping La further inhibits the agglomeration, growth and crystallization of TiO_2 nanoparticles. As shown in Table 3, these particles are smaller than 7 nm, much smaller than the counterparts doped with Zn only.

Table 4 shows the XPS characterization results of co-doped TiO_2. The surface concentration of Zn and La are both higher than the defined values, confirming that both of them are dispersed on the surface of TiO_2 nanoparticles. It also shows that the content of surface-bound OHs gradually decreases when the amount of La is increased. Specifically, the content of OHs of 7%La–1%Zn/TiO_2 is similar to that of naked TiO_2. These results suggest that doping La suppresses the formation of surface-bound OHs.

Fig. 8 shows the UV–vis spectra of co-doped nanoparticles. Compared with Zn-doped sample, the co-doped samples show obvious blue shift. The maximum absorption and absorption band edge are about 316 nm and 390 nm, respectively. At the same time, the absorption in <390 nm region is significantly enhanced. This may be attributed to the quantum-size effect

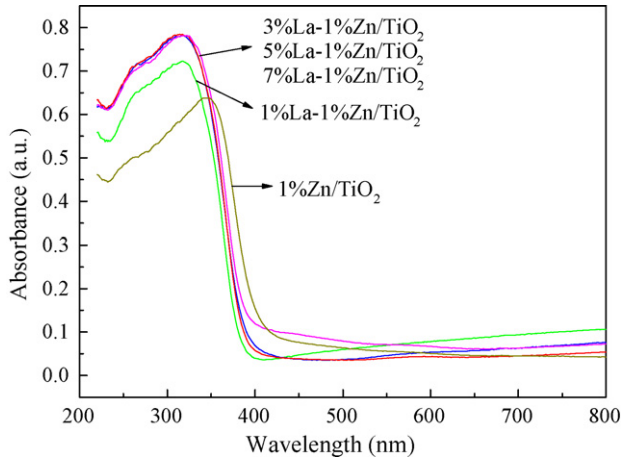

Fig. 8. Optical absorption of La and Zn co-doped TiO_2 calcined at 500 °C.

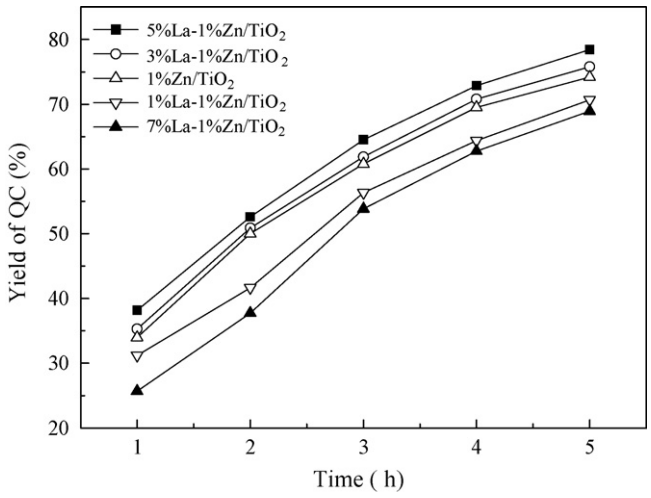

Fig. 9. Photocatalytic activity of La and Zn co-doped TiO_2 calcined at 500 °C.

of nanoparticles [28], consistent with the results in Table 3. When the amount of La exceeds 3%, the samples show identical absorption because they have very similar particle size.

3.2.2. Photoactivity

Fig. 9 shows the yield of QC over co-doped TiO_2 nanoparticles. Doping 5% and 3% La further improve the photoactivity of Zn-doped TiO_2. This is attributed to the quantum-size effect that induces significantly high optical absorption in UV region and high efficiency in charge separation and transfer.

It is noted that doping 1% and 7% La is detrimental to the photocatalytic reaction. The sample doped with 7% La has similar particle size and optical absorption compared with the counterparts doped with 3% and 5% La. The only difference between them is the content of surface-bound OHs. Therefore, the low activity of 7%La–1%Zn/TiO_2 is caused by the lack of OHs, which confirms that the surface-bound OHs are very important for the isomerization of NBD. Although 1%La–1%Zn/TiO_2 has the highest content of OHs, it shows much weaker optical absorption, thus exhibiting a low activity. This indicates that optical absorption is another important factor influencing the activity. In summary, for the La and Zn co-doped nanoparticles, the role of Zn is to increase the content of surface-bound OHs, whereas La is to reduce the particle to quantum-size at the expense of surface-bound OHs. Therefore, the amounts of Zn and La have to be carefully chosen to obtain a good balance between these two properties.

3.3. Possible isomerization mechanism over semiconductors

In a concise technical note, Lahiry and Haldar reported that semiconductors including ZnO, ZnS and CdS could facilitate the photocatalytic isomerization of NB to QC [15]. It was declared that this reaction only occurred with the presence of O_2, and no QC was produced under evacuated conditions. They presented a mechanism involving the weakly negative $O_2^{\bullet}$. However, our work shows that O_2 has no obvious influence on this reaction, thus the proposed mechanism seems not suitable for the present

case. Also, the triplet state isomerization mechanism (see Section 1) seems not suitable because the vertical triplet energy transfer from semiconductor to reactant is very difficult.

The present study indicates that the isomerization reaction over semiconductors should be closely related to the photoinduced holes, especially, the holes trapped by surface-bound OHs. The free radical ion isomerization mechanism is ruled out because the energy of free $NBD^{\bullet+}$ is significantly lower than free $QC^{\bullet+}$. In fact, the transformation of QC to NBD is via the $QC^{\bullet+} \rightarrow NBD^{\bullet+}$ free radical route [29]. Therefore, the reaction is very likely to occur through an exciplex (charge-transfer) intermediate [13]

$$TiO_2 - OH \xrightarrow{h\nu} TiO_2{}^- - OH^+ \quad (1)$$

$$TiO_2{}^- - OH^+ + NBD \rightarrow TiO_2{}^- - OH\cdots NBD^+ \quad (2)$$

$$TiO_2{}^- - OH\cdots NBD^+ \rightarrow TiO_2{}^- - OH\cdots QC^+ \quad (3)$$

$$TiO_2{}^- - OH\cdots QC^+ \rightarrow TiO_2 - OH + QC \quad (4)$$

The photoinduced holes in the valance band are trapped by the surface-bound OHs (Eq. (1)). NBD molecules are absorbed on the charged surface-bound OHs, and simultaneously the charge is transferred to NBD molecules (Eq. (2)). Then positively charged NBD species undergoes isomerization to form QC species (Eq. (3)). Finally the charge is recombined through back electron transfer and QC molecules are desorbed (Eq. (4)). In this process, the charge-transfer intermediate can stabilize the charged NBD and QC species, and the surface-bound OHs and charge separation efficiency (quantum-size effect) are two key factors.

4. Conclusion

Zn- and La-doped TiO_2 nanoparticles have been synthesized for the photocatalytic isomerization of norbornadiene to quadricyclane. Zn ions mainly distribute on the surface of doped-TiO_2 in the form of ZnO crystallites, instead of substituting the lattice Ti ions. These crystallites can inhibit the agglomeration and anatase-to-rutile phase transformation, resulting in smaller particles with excellent thermal stability. The surface-bound OHs of the particles are greatly increased by doping Zn. 1%Zn/TiO_2 shows the best photocatalytic performance due to the highest content of surface-bound OHs. Doping La on 1%Zn/TiO_2 further reduces the particle to quantum-size, causing obvious blue-shifted and sharply increased optical absorption. Nevertheless, the formation of surface-bound OHs is suppressed. 5%La–1%Zn/TiO_2 and 3%La–1%Zn/TiO_2 shows significantly high activity due to a good balance between the quantum-size effect and the content of surface-bound OHs.

Acknowledgement

The support from fundamental research project of COSTIND (A1420060192) is greatly appreciated.

References

[1] R. Marzio, S. Antonio, F. Federico, F. Carlo, Inorg. Chem. 38 (1999) 1520–1522.
[2] A.D. Dubonosov, V.A. Bren, V.A. Chernoivnov, Russ. Chem. Rev. 71 (2002) 917–927.
[3] M.Z. Kassaee, E. Vessally, J. Mol. Struct. Theochem. 716 (2005) 159–163.
[4] C. Philippopoulos, D. Economou, C. Economou, J. Marangozls, Ind. Eng. Chem. Prod. Res. Dev. 22 (1983) 627–633.
[5] S.D. Bai, P. Dumbacher, J.W. Cole, NASA/TP-2002-211729.
[6] T. Kokan, Characterizing high-energy-density propellants for space propulsion applications, PhD Dissertation, Georgia Institute of Technology, 2007.
[7] R. Nichols, T.A. Mckelvey, S. L. Rodgers, US Patent 5,616,882 (1997).
[8] S.J. Schneider, US Patent 6,311,477 (2001).
[9] T. Akioka, Y. Inoue, A. Yanagawa, M. Hiyamizu, Y. Takagi, A. Sugimori, J. Mol. Catal. A: Chem. 202 (2003) 31–39.
[10] P.A. Grutsh, C. Kutal, J. Am. Chem. Soc. 108 (1986) 3108–3110.
[11] A. Cuppoletti, J.P. Dinnocenzo, J.L. Goodman, I.R. Gould, J. Phys. Chem. A 103 (1999) 11253–11256.
[12] V.A. Petrov, N.V. Vasil'ev, Curr. Org. Synth. 3 (2006) 215–259.
[13] G.W. Sluggett, N.J. Turro, H.D. Roth, J. Phys. Chem. A 101 (1997) 8834–8838.
[14] P. Cahill, R.N. Steppel, U.S. Patent 6,635,152 (2003).
[15] S. Lahiry, C. Haldar, Solar Energy 37 (1986) 71–73.
[16] M.R. Hoffmann, S.T. Martin, W. Choi, D.W. Bahnemann, Chem. Rev. 95 (1995) 69–96.
[17] A.L. Linsebigler, G. Lu, J.T. Yates Jr., Chem. Rev. 95 (1995) 735–758.
[18] J.J. Zou, H. Hei, C. Lan, H.Y. Hai, Int. J. Hydrogen Energy 32 (2007) 1762–1770.
[19] G. Liu, X. Zhang, Y. Xu, X. Niu, L. Zheng, X. Ding, Chemosphere 59 (2005) 1367–1371.
[20] L. Jing, B. Xin, F. Yuan, L. Xue, B. Wang, H. Fu, J. Phys. Chem. B 110 (2006) 17860–17865.
[21] A.-W. Xu, Y. Gao, H. Liu, J. Catal. 207 (2002) 151–157.
[22] L. Jing, X. Sun, B. Xin, B. Wang, W. Cai, H. Fu, J. Solid State Chem. 177 (2004) 3375–3382.
[23] Y. Xie, Y. Li, X. Zhao, J. Mol. Catal. A: Chem. 277 (2007) 119–126.
[24] J.C. Colmenares, M.A. Aramendía, A. Marinas, J.M. Marinas, F.J. Urbano, Appl. Catal. A: Chem. 306 (2006) 120–127.
[25] Y. Huo, J. Zhu, J. Li, G. Li, H. Li, J. Mol. Catal. A: Chem. 278 (2007) 237–243.
[26] J. Tang, H. Quan, J. Ye, Chem. Mater. 19 (2007) 116–122.
[27] J. Zhang, M. Li, Z. Feng, J. Chen, C. Li, J. Phys. Chem. B 110 (2006) 927–935.
[28] Z. Zhang, C.-C. Wang, R. Zakaria, J.Y. Ying, J. Phys. Chem. B 102 (1998) 10871–10878.
[29] H. Ikezawa, C. Kutal, J. Org. Chem. 52 (1987) 3299–3303.